Journal of Cellular and Molecular Medicine
A JOURNAL OF TRANSLATIONAL MEDICINE

J. Cell. Mol. Med. Vol 16, No 1, 2012 pp. 59-71

Proteomic analysis of metabolic, cytoskeletal and stress response proteins in human heart failure

Weiming Li [a, #], Rong Rong [b, #], Sheng Zhao [c, #], Xiaoming Zhu [a], Ke Zhang [d], Xin Xiong [e], Xueqing Yu [b], Qinghua Cui [f], Shuqiang Li [g], Li Chen [h], Jun Cai [a, *], Jie Du [i, *]

[a] *Department of Cardiology, Chaoyang Hospital, The Key Laboratory of Remodelling-related Cardiovascular Diseases, Capital Medical University, Ministry of Education, Beijing, China*
[b] *Department of Nephrology, The First Affiliated Hospital of Sun Yat-Sen University, Guangzhou, China*
[c] *Department of Cardiac Surgery, The First Affiliated Hospital of Nanjing Medical University, Nanjing, China*
[d] *German Research Center for Environmental Health, Technische Universität München, München, Germany*
[e] *The First Affiliated Hospital, Chongqing Medical University, Chongqing, China*
[f] *Department of Biomedical Informatics, Peking University Health Science Center, Beijing, China*
[g] *Department of Cancer Immunology and AIDS, Dana-Farber Cancer Institute, Harvard Medical School, Boston, MA, USA*
[h] *Texas Heart Institute, Houston, TX, USA*
[i] *Beijing Anzhen Hospital Affiliated to the Capital Medical University, The Key Laboratory of Remodelling-related Cardiovascular Diseases, Capital Medical University, Ministry of Education, Beijing, China*

Received: March 3, 2011; Accepted: April 27, 2011

Abstract

Human heart failure is a complex syndrome and a primary cause of morbidity and mortality in the world. However, the molecular pathways involved in the remodelling process are poorly understood. In this study, we performed exhaustive global proteomic surveys of cardiac ventricle isolated from failing and non-failing human hearts, and determined the regulatory pathway to uncover the mechanism underlying heart failure. Two-dimensional gel electrophoresis (2-DE) coupled with tandem mass spectrometry was used to identify differentially expressed proteins in specimens from failing ($n = 9$) and non-failing ($n = 6$) human hearts. A total of 25 proteins with at least 1.5-fold change in the failing heart were identified; 15 proteins were up-regulated and 10 proteins were down-regulated. The altered proteins belong to three broad functional categories: (i) metabolic [*e.g.* NADH dehydrogenase (ubiquinone), dihydrolipoamide dehydrogenase, and the cytochrome *c* oxidase subunit]; (ii) cytoskeletal (*e.g.* myosin light chain proteins, troponin I type 3 and transthyretin) and (iii) stress response (*e.g.* αB-crystallin, HSP27 and HSP20). The marked differences in the expression of selected proteins, including HSP27 and HSP20, were further confirmed by Western blot. Thus, we carried out full-scale screening of the protein changes in human heart failure and profiled proteins that may be critical in cardiac dysfunction for future mapping.

Keywords: heart failure • proteomics • metabolism • cytoskeleton • heat shock protein

Introduction

Heart failure, a complex syndrome that leads to left ventricular systolic and diastolic dysfunction, is one of the main causes of morbidity and mortality in the world [1]. Despite considerable recent research effort regarding its genetic causes, heart failure prevention and treatment strategies still suffer significant limitations [2]. Proteins, the products of gene expression, are the essential

[#]These authors contributed equally to this work.
*Correspondence to: Jun CAI, M.D.,
Department of Cardiology, Chaoyang Hospital,
Capital Medical University, Beijing 100020, China.
Tel.: +86-10-85231937
Fax: +86-10-65951064
E-mail: caijun7879@yahoo.com.cn.

Jie DU, Ph.D.,
Beijing Institute of Heart,
Lung and Blood Vessel Diseases,
Beijing 100029, China.
Tel.: +86-10-64456030
Fax: +86-10-64451050
E-mail: jdu@bcm.edu

doi:10.1111/j.1582-4934.2011.01336.x

biological determinants of disease phenotype, and changes in endogenous and external stimulation result in changes in the proteomes of individual patients over time. It is the proteomics, not the genome, that reveal the details within a cell [3]. One goal of functional proteomics is to examine global protein expression to elucidate the functional role of proteins and provide new insights into cellular mechanisms. This establishes the link between a cellular/organ proteome and the genesis of a physiological/pathological phenotype, which presents the investigator with new opportunities.

The central goal of this study is to delineate changes in protein expression between failing and non-failing human hearts and define the regulatory pathway to uncover the mechanism. Two-dimensional gel electrophoresis (2-DE) profiling techniques, which promised to resolve several thousand proteins in a single myocardial tissue sample, were used to examine changes in protein expressions and to identify key molecular players involved during disease progression. At the same time, our establishment of the proteomic map of human myocardium further revealed and provided the fundamental basis for the mechanism of heart failure.

Table 1 Clinical characteristics of patients with heart failure

ID	Sex	Age	Disease	LVEF (%)	Drug therapy
No. 1	M	33	DCM	14	DIG, ACEI
No. 2	F	45	DCM	35	ACEI, BB
No. 3	M	43	DCM	34	AMIO, ACEI
No. 4	M	39	DCM	35	BB, ACEI
No. 5	M	57	DCM	33.9	ACEI, AMIO
No. 6	M	38	DCM	31.7	DIG, ACEI
No. 7	M	48	DCM	30.4	ACEI, BB
No. 8	M	42	DCM	26.3	DIG, DOB
No. 9	F	50	DCM	35	ACEI, AMIO

F: female; M: male; LVEF: left ventricular ejection fraction measured prior to explant; DCM: dilated cardiomyopathy (pre-transplant diagnosis); Drug Therapy: DIG: digoxin; DOB: dobutamine; AMIO: amiodarone; ACEI: angiotensin-converting enzyme inhibitor (usually lisinopril); BB: β-adrenergic blocker (metoprolol or carvedilol).

Materials and methods

Patient samples

Tissues for proteomic analysis were collected from the left ventricular free wall which was obtained from explanted hearts of transplant recipients ($n = 9$) with a diagnosis of dilated cardiomyopathy (DCM, EF $\leq$ 35%) and non-failing control hearts ($n = 6$) which were obtained from unmatched donors whose hearts were not suitable to transplantation. The baseline characteristics of patients are displayed in Table 1. The hearts were arrested and transported in ice-cold, oxygenated cardioplegic solution. Once in the laboratory the tissue was flash frozen in liquid N_2 and stored at -80°C. The study protocol was approved by the Medical Ethical Committee of the Chaoyang Hospital of Capital Medical University.

Whole protein extraction

Tissue was homogenized by a Polytron PT-MR2100 (Kinemetica AG, Switzerland) in lysis buffer (7M urea, 2M thiourea, 4% CHAPS, 2% IPG buffer pH 4–7 linear, 40 mM Tris, 65 mM DTT). Homogenates were immediately placed on ice to inhibit proteolysis, and then centrifuged at 14,000 rpm at 4°C for 30 m. The supernatant was collected and transferred to a new tube. The protein was stored in aliquots at -80°C until analysis. Protein samples were quantified using the Bradford protein quantitative method.

Two-dimensional gel electrophoresis

2-DE was performed according to the manufacturer's instructions (GE Healthcare, Piscataway, NJ, USA). Briefly, each protein sample in the lysis buffer was diluted to 450 μl with rehydration solution (9M urea, 2% CHAPS, 30 mM DTT, 0.5% IPG buffer pH 4–7, 0.002% bromphenol blue). Immobiline DryStrip gels (pH 4–7, 24 cm; GE Healthcare) were rehydrated with 450 μl of mixture solution in 24-cm strip holders and electrofocused with an Ettan IPGphor Isoelectric Focusing System (GE Healthcare). The focusing protocol was performed as follows: 50 μA/strip at 20°C, 30 V for 6 hrs, 500 V for 1 hr, 1000 V for 3 hrs, 3000V for 2 hrs, 5000 V for 2 hrs and 10,000 V for 8.5 hrs. Equilibrated IPG strips were placed at self-cast large-format 13% gradient polyacrylamide gels (255 × 196 × 1 mm) and embedded with 0.5% agarose, 0.001% bromophenol blue in cathode-running buffer (192 mM glycine, 24.8 mM Tris, 0.1% SDS, pH 8.3). Proteins were separated in the second dimension by SDS-PAGE using Ettan DALT 12n electrophoresis system (Amersham LifeSciences, Arlington Heights, IL, USA) containing cathode-running buffer at a regulated temperature of 16°C by a cooling unit. The gels were run at 2 W per gel for the initial 30 m followed by 12 W per gel until the bromophenol blue dye front reached the bottom of the gel (total duration 6 and 7 hrs). All samples were run in triplicate.

Protein visualization, imaging analysis and in-gel trypsin digestion

All protein spots in 2-D gels were visualized by Coomassie Blue R-350 staining (Amersham Biosciences). Other standard chemicals required were purchased from Sigma-Aldrich (St. Louis, MO, USA). Stained gels were scanned on an Image-Scanner (Amersham Biosciences), and images were analysed with ImageMaster 2D 7.0 software supplied by the manufacturer. A total of 45 gel images were used for analysis. On average, over 1000 spots were detected on each 2-D gel image. Among these, about 950 of the most reproducible spots were included in the data analysis. Protein spots separated on 2-D gels were quantitated in terms of their relative volume (spot volume/total spot volume). For comparison, one image was chosen and allocated as the reference gel to align all other images in the experiment. Following manual alignment, spot detection, background subtraction and normalization were performed. To normalize the expression data, the data from one sample were fixed and all other samples were calibrated to this reference. Only those spots with a twofold or greater changes in expression levels were considered significant and selected for spot picking, trypsin digestion and mass spectrometry analysis to identify their protein content.

Protein spots demonstrating different expression patterns compared with controls were excised from gels by hand, and processed for mass spectrometric analysis. Excised spots were digested (9 hrs) *in situ* with trypsin. Peptides were extracted by addition of a 50% acetonitrile, 5% trifluoroacetic acid (TFA) solution and extracted solutions were concentrated to 4 μl in a lyophilizer (LABCONCO Freezone Liter; Labconco Corporation, Kansas City, MO, USA). A protein-free gel piece was similarly processed and used as the control to identify autoproteolysis products derived from trypsin.

Mass spectrometry analysis and database searching

The digested samples were spotted onto a MADLI target with an equal volume of cyano-4-hydroxycinnamic acid (2 mg/ml; Bruker Daltonics, Bremen, Germany) saturated with 70% acetonitrile in 0.1% TFA. They were analysed by MALDI-TOF MS using an AutoFlex TOF/TOF II mass spectrometer (Bruker Daltonics). The instrument settings were positive ion reflection mode, an accelerating voltage of 20 kV, and 150-ns delayed extraction time. The spectrum masses were ranged from 800 to 4000 Da and acquired with laser shots at 100/spectrum. A Peptide Mixture-1 kit (Bruker Daltonics) was used for external calibration. The matrix and autolytic peaks of trypsin were used as internal standards for mass calibration. Monoisotopic mass was analysed with FlexAnalysis 2.0 (Bruker Daltonics) and automatically collected with a signal-to-noise ratio > 4 and a peak quality index > 30. The known contaminant ions (human keratin and tryptic autodigest peptides) were excluded. For interpretation of the mass spectra, monoisotopic peptide masses were searched on Mascot (http://www.matrixscience.com/cgi/search_form.pl?FORMVER = 2&SEARCH = PMF) for protein identity searching.

Many of processed spectra from the AutoFlex MALDI-TOF/TOF II mass spectrometer were searched against the NCBI nonredundant protein database (updated on January 28, 2010), which contained 10,348,164 sequences. The search was restricted to 'Homo sapiens (human)' as taxonomy, which contained 229,313 sequences. The other main search parameters for all peptide mass fingerprinting searches were as follows: type of search, peptide mass fingerprint; enzyme, trypsin; fixed modifications, carbamidomethylcysteine; variable modifications, oxidation (M); mass values, monoisotopic; protein mass, unrestricted; peptide mass tolerance, 100 p.p.m.; fragment mass tolerance, ±0.3 Da; peptide charge state, 1+ and maximum missed cleavages, 1. Proteins whose scores were greater than 66 were considered significant ($P < 0.05$).

Ingenuity pathways analysis

Ingenuity pathways analysis (IPA; Ingenuity Systems®, http://www.ingenuity.com) is a web-based application that enables the visualization, discovery and analysis of molecular interaction networks. The functional analysis identified the biological functions and/or diseases that were most significant to the data sets. Fisher's exact test was performed to calculate a *P* value determining the probability that each biological function and/or disease assigned to the data set was due to chance alone. Networks of the altered proteins were algorithmically generated based on their connectivity.

Western blot analysis

Proteins were extracted from human hearts as described, and then Western blot analysis was performed. Protein expression was evaluated by incubating membranes in 1:1000 rabbit polyclonal antibody (Abcam, San Francisco, CA, USA), followed by incubation with a 1:5000 secondary antibody (anti-rabbit IgG, HRP linked). Proteins were detected using the Fuji 3000 Image Station system. Protein blots were quantitated by densitometry using the Image J software program.

Gene expression microarray

Total RNA was extracted from heart tissues using Trizol reagent (Invitrogen, Carlsbad, CA, USA), according to the manufacturer's instructions. RNA samples were labelled using the Illumina labelling kit and hybridized on the Human WG-6-v3 BeadChip Array. Scanning was performed with the Illumina's iScan scanner. GenePix pro V6.0 was used to read the raw intensity of the image. Perfect match fluorescence intensities were background-corrected, mismatch-adjusted, normalized and summarized to yield $\log_2$-transformed gene expression data using the GCRMA algorithm. The threshold value we used to define up-regulated and down-regulated mRNAs was a fold change greater than 1.5, and *P* value < 0.05 calculated by *t*-test.

Real-time reverse transcriptase-polymerase chain reaction (RT-PCR)

Total RNA was extracted from tissues by using Trizol reagent (Invitrogen), and cDNA was synthesized with Superscript II (Invitrogen) in accordance with the manufacturer's instructions. Selected mRNAs (HSP27 and HSP20) were quantified with TaqMan quantitative RT-PCR. Primers for HSP20: 5′-CGTGGAGGTGCACGCG-3′, 3′-GCGACGGTGGAACTC GC-5′, probe: FAM-AGCGCCCGGATGAGCACG-BHQ1; Primers for HSP27: 5′-GATGAAGCTGT-CACTCGAGGC-3′, 3′-CCATCTCAGAGATATTGGATATGGT-5′, probe: FAM-TGTGCATTGCAGTGTGCCATCTTATC-BHQ1. The PCRs were carried out in a final volume of 20 μl using a 7500 Real-Time PCR System (Applied Biosystems). Reactions consisted of 1.33 μl cDNA, TaqMan Universal PCR Master mix (Applied Biosystems), 0.2 μM TaqMan Probe, 1.5 μM forward primer and 0.7 μM reverse primer. The PCRs were initiated with a 10-min. incubation at 95°C followed by 40 cycles of 95°C for 15 sec. and 60°C for 60 sec. The expression levels of mRNAs were normalized to internal control β-actin and were calculated utilizing the ΔΔCt method.

Statistical analysis

In this study, more than 1.5-fold increase or decrease protein was cut-off to distinguish changes and analysis. Data are expressed as mean ± S.D. All statistical analyses were performed with SPSS version 13.0. Functional data were analysed using analysis of variance (with repeated measures and the Tukey test for pairwise comparisons) and the Student's *t*-test (with Bonferroni correction), as appropriate. All statistical calculations utilized Microsoft Excel software. Statistical significance was set at $P < 0.05$.

Results

Differential protein expression analysis of failing and non-failing human hearts

A total of 45 2-D gels were used in the differential proteomic analysis. The protein profile between replicate gels and biological

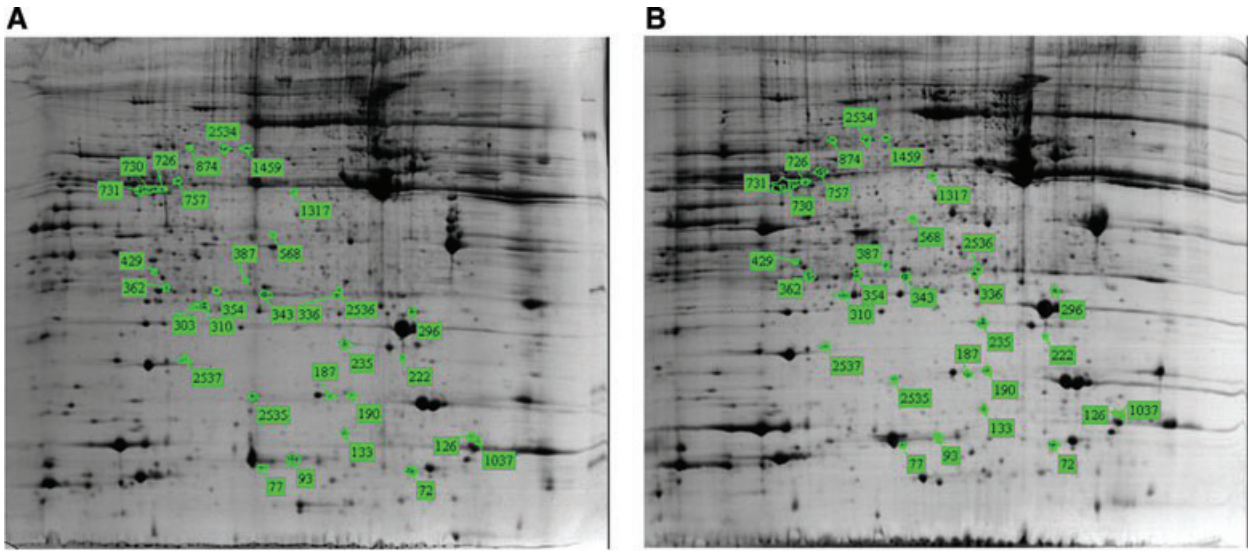

Fig 1. Image of a two-dimensional gel running a sample of human LV tissue, depicting localisation of proteins according to their molecular weight and pH. Twenty-five protein spots were identified as differentially expressed in three-way comparison of heart failure (**A**) and normal groups (**B**), respectively.

samples showed high similarities, and the spot pattern was observed to be comparable between two groups. Image analysis of 2-D gels from all samples detected a total of 1000 protein spots. A total of 25 protein spots showed at least 1.5-fold difference in the normal controls (non-failing human hearts) *versus* disease samples (Fig. 1). The total 25 protein spots (15 increased, 10 decreased; Tables 2 and 3) were also observed to have differentially expressed at least a 1.5-fold change in the three-way pairwise comparisons, which were obtained by liquid chromatography-mass spectrometry/mass spectrometry. Classification of these proteins using the LOCATE subcellular localization database [4] showed that the majority of differentially expressed proteins comprised macromolecular (40%), cytoskeletal (28%) and mitochondrial (28%) proteins (Fig. 2A). PANTHER classification [5] of proteins by biological process revealed that the majority of proteins were involved in protein binding (cell structure and muscle contraction), ion binding (calcium binding) and hydrolase activity (Fig. 2B). The spots of most interest were those observed to have expression-level changes in comparison of normal *versus* failing hearts. These different proteins participate in some important biological process categories, such as multi-cellular organismal processes, biological regulation, developmental processes, metabolic processes and response to stimulus (Fig. 2C). The distribution and function of these expressed proteins provide a link to molecular components and pathways that may be involved in the development of heart failure progression. The findings suggest that major protein changes in human heart failure pathogenesis can be grouped into three main categories: proteins involved in mitochondria and energy production, cytoskeletal proteins and binding proteins. Therefore, the pathology of the failing heart is characterized by reduced mitochondrial activity, disruption of energy production and loss of cardiomyocytic structural integrity.

The network of proteomics

To characterize the functions associated with the detected proteins, the protein list was uploaded into the IPA software server and analysed using the Core Analysis module per the manufacturer's instructions (http://www.ingenuity.com). As seen in Figure 3, the proteins are most significantly related to cardiovascular diseases and organism injury and abnormalities, which suggests that the proteins detected in this study is mostly regulators/effectors of the progression of heart failure.

As shown in Figure 4, the proteins mentioned before constitute the main structure of the regulation network. They all participate in the process of heart failure connected by important modulators, such as NF-κB, Myc and P38-MAPK, in respective pathways [6–8]. Besides, several metabolism disease pathways, including Growth Hormone and PRDX6, were also highlighted [9]. Meanwhile, functional modules related to cell differentiation and proliferation, as well as apoptosis were centred in the interaction network including only experimentally validated targets. Moreover, some important modulators in immune/inflammatory response, cardiovascular development or angiogenesis, such as TTR, ANGPT2 and FABP can also be found in the interaction map [10–12]. Therefore, the altered expression of those key proteins may cause the acceleration or deference of the heart failure process.

Western blot analysis

Western blot analysis was used to confirm significant protein expression changes observed in the 2-D gel proteomic data. Immunoblotting for the 27-kD heat shock protein (HSP27) band confirmed a marked difference in protein expression in the context

Table 2 Identification of up-regulated proteins (≥1.5-fold) in failing *versus* normal hearts

Spot no.	Symbol	Gene name	Subcellular location	Molecular function	Biological process	Fold change
2535	HSP20 (HSPB6)	Heat shock protein, α-crystallin-related, B6	Cytoplasm	Protein binding; protein homodimerization activity	Regulation of muscle contraction	4.65
93	COX5B	Cytochrome *c* oxidase subunit Vb	Mitochondrion	Cytochrome *c* oxidase activity; metal ion binding	Respiratory gaseous exchange	6.07
2537	CRYAB	Crystallin, αB	Cytoplasm/ nucleus	Microtubule binding; cytoskeletal protein binding; protein homodimerization activity; unfolded protein binding	Glucose metabolic process; oxygen and reactive oxygen species metabolic process; muscle contraction; response to hydrogen peroxide	2/1
72	LGALS1	Lectin, galactoside-binding, soluble, 1	Extracellular space	Glycoprotein binding; signal transducer activity; protein binding; galactoside binding	Apoptosis; positive regulation of I-κB kinase/NF-κB cascade; myoblast differentiation	2
126	MYL2	Myosin, light chain 2, regulatory, cardiac, slow	Cytoskeleton	Actin monomer binding; calcium ion binding; protein binding; structural constituent of muscle; myosin heavy chain binding	Regulation of striated muscle contraction; negative regulation of cell growth; cardiac myofibril assembly; ventricular cardiac muscle tissue morphogenesis; heart contraction	2.4
222	HSPB2	Heat shock 27 kD protein 2	Cytoplasm	Protein binding; enzyme activator activity	Response to unfolded protein; somatic muscle development	2
1037	MYL6	Myosin, light chain 6, alkali, smooth muscle and non-muscle	Cytoskeleton	Motor activity; calcium ion binding; structural constituent of muscle; actin-dependent ATPase activity	Muscle contraction; skeletal muscle tissue development; muscle filament sliding	3.07
874	DLD	Dihydrolipoamide dehydrogenase	Mitochondrion / cytoplasm	Dihydrolipoyl dehydrogenase activity; oxidoreductase activity; lipoamide binding; FAD binding; NAD or NADH binding	Acetyl-CoA biosynthetic process from pyruvate; mitochondrial electron transport, NADH to ubiquinone	1.5
1459	OXCT1	3-Oxoacid CoA transferase 1	Mitochondrion	Transferase activity; protein homodimerization activity	Metabolic process; cellular ketone body metabolic process; ketone body catabolic process	2.25
77	FABP4	Fatty acid binding protein 4, adipocyte	Cytoplasm/ nucleus	Fatty acid binding; protein binding; transcription repressor activity	Negative regulation of protein kinase activity; fatty acid metabolic process	2.08
336	PRDX6	Peroxiredoxin 6	Cytoplasm/ nucleus	Antioxidant activity; oxidoreductase activity; hydrolase activity	Response to oxidative stress; phospholipid catabolic process; lipid catabolic process	2
2534	HSPA2	Heat shock 70 kD protein 2	Cytoplasm/ mitochondrion	Nucleotide binding; ATP binding; unfolded protein binding	Response to unfolded protein	2.53
354	TNNI3	Troponin I type 3 (cardiac)	Cytoplasm	Actin binding; calcium channel inhibitor activity; protein kinase binding; troponin C binding; troponin T binding; calcium-dependent protein binding	Regulation of systemic arterial blood pressure by ischaemic conditions; cellular calcium ion homeostasis; regulation of smooth muscle contraction; negative regulation of ATPase activity; cardiac muscle contraction	2
133	TTR	Transthyretin	Extracellular space	Transporter; hormone activity; protein binding	Regulation of systemic arterial blood pressure by ischaemic conditions; cellular calcium ion homeostasis; negative regulation of ATPase activity; cardiac muscle contraction	1.56
343	HSP27 (HSPB1)	Heat shock 27 kD protein 1	Cytoplasm	Protein binding; ubiquitin binding	Cellular component movement; response to unfolded protein; response to heat	2.1

Table 3 Identification of down-regulated proteins (≥1.5-fold) in failing *versus* normal hearts

Spot no.	Symbol	Entrez Gene name	Subcellular location	Molecular function	Biological process	Fold change
190	BCL2A1	BCL2-related protein A1	Cytoplasm	Protein binding	Regulation of apoptosis; anti-apoptosis	−2.3
730	CKM	Creatine kinase, muscle	Cytoplasm	Kinase	Creatine metabolic process; phosphocreatine biosynthetic process	−2
1317	IFIH1	Interferon induced with helicase C domain 1	Cytoplasm/ nucleus	Nucleotide binding; helicase activity; protein binding; ATP binding; hydrolase activity	Regulation of apoptosis; innate immune response	−2
568	KRT9	Keratin 9	Cytoskeleton	Structural constituent of cytoskeleton; protein binding	Epidermis development; skin development; intermediate filament organization	−2.63
387	DCI	Dodecenoyl-Coenzyme A delta isomerase (3,2 trans-enoyl-Coenzyme A isomerase)	Mitochondrion	Isomerase activity	Lipid metabolic process; fatty acid metabolic process	−1.5
2536	NDUFS3	NADH dehydrogenase (ubiquinone) Fe-S protein 3, 30 kD (NADH-coenzyme Q reductase)	Mitochondrion	Protein binding; NADH dehydrogenase (ubiquinone) activity; electron carrier activity	Mitochondrial electron transport, NADH to ubiquinone; oxygen and reactive oxygen species metabolic process; transport; induction of apoptosis; electron transport chain; negative regulation of cell growth	−2
235	PRDX2	Peroxiredoxin 2	Cytoplasm	Antioxidant activity; oxidoreductase activity	Negative regulation of oxygen and reactive oxygen species metabolic process; negative regulation of lipopolysaccharide-mediated signaling pathway	−1.51
187	SRP19	Signal recognition particle 19 kD	Cytoplasm/ nucleus	7S RNA binding	Cotranslational protein targeting to membrane; SRP-dependent cotranslational protein targeting to membrane	−2.36
296	MYL4	Myosin, light chain 4, alkali; atrial, embryonic	Cytoskeleton	Actin monomer binding; calcium ion binding; structural constituent of muscle; myosin II heavy chain binding; actin filament binding	Regulation of the force of heart contraction; muscle organ development; positive regulation of ATPase activity; cardiac muscle contraction	−1.5
310	UQCRFS1	Ubiquinol-cytochrome *c* reductase, Rieske iron-sulphur polypeptide 1	Mitochondrion	Oxidoreductase activity, metal ion binding; 2 iron, 2 sulphur cluster binding	Transport; electron transport chain; response to drug; oxidation reduction	−2.15

of heart failure. After normalization for loading differences, a four-fold change was detected ($P = 0.0012$; Fig. 5A and B). Immunoblotting for the 16-kD HSP20 band is also differently expressed in the context of heart failure; an approximately three-fold change was detected in the heart failure group compared with the non-failing group ($P = 0.0029$; Fig. 5C and D). Also, other six proteins were randomized selected for Western blot, including CRYAB, CKM, TNNI3, MYL2, COX5B and TTR. The results were coincident with proteomic analysis (Fig. 6).

Merging proteomics and gene expression signatures

Integration of proteomics with gene expression profiling would be more informative than either platform alone in capturing differentially involved gene networks between heart functional subtypes. Hierarchical cluster analysis of 741 significantly differentially expressed genes successfully segregates heart failure disease from healthy controls (Fig. 7). To identify a core set of functionally relevant genes/proteins, we explored the overlap of the differentially

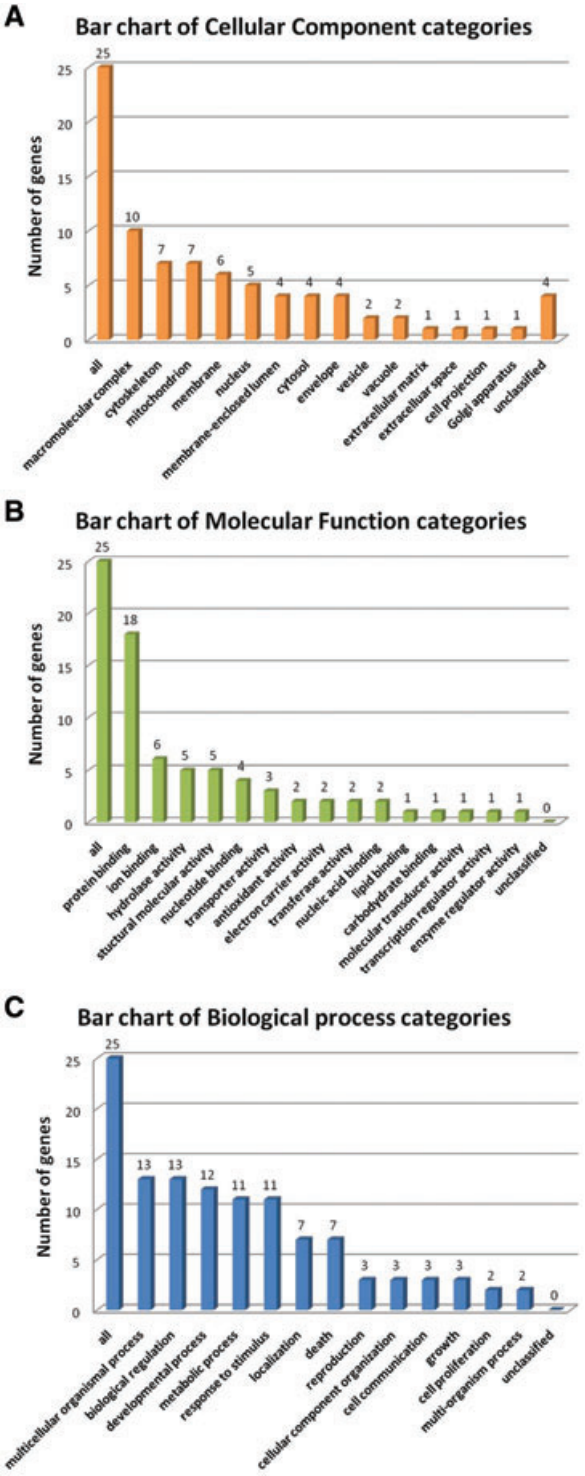

Fig. 2 Functional classification of proteomic data by bioinformatic analysis. Bar chart represents the cellular component categories (**A**), the molecular function categories (**B**) and the biological process categories (**C**). Categorizations are based on information provided by the online curated resource LOCATE subcellular localization database and PANTHER classification system.

regulated gene/protein sets captured by gene expression (741 genes) and global proteomic surveys (25 proteins) and represented on both arrays. There was just one protein, HSPA2, presented in gene expression signature, suggesting that the regulation of the most of altered proteins occurred at the level of post-transcription (Table 4). Furthermore, we performed validation experiments to verify the expression data from the microarrays. There are no significant differences of the mRNA expression of HSP27 and HSP20, between failed and non-failed group by quantitative RT-PCR (Fig. 8).

Discussion

The strategies available to prevent or treat heart failure are ineffective, which is due to the lack of a fundamental understanding of the cause and pathophysiology of the disorder. This study provides several intriguing findings. First, we identified a novel protein pattern in the failed human hearts, which may become helpful for the diagnosis and prognosis of patients with heart failure. Furthermore, we evaluated the global protein expressions to elucidate the functional role of network proteins and provide new information for cellular mechanisms, complement to other investigations with cultured heart cells or animal studies [13–15]. In addition, a protein network was set up to show the relationship between pathological changes in protein expression and integrated interactions with other known functionally linked proteins that may precipitate heart failure, providing the basis for further research.

In this study, we have shown that 741 genes were dysregulated in failed hearts identified by mRNA microarray. Interestingly, dysregulated proteins identified by proteomics did not correlate well with dysregulated gene expression profile. Several possibilities may account for the discrepancy, for example, it could be due to the transcriptional efficiency, protein stability, post-transcriptional modulation and/or alteration of the ubiquitin–proteasome system [16–18]. It could also resulted from the time course differences in transcription and pathological processes, the dysregulated proteins in failed heart may be expressed at prior stage, suggesting it will be ideally to detect mRNA expression profile at early stage of heart failure in the future study.

The proteins expressed in failing hearts were first investigated over a decade ago in a mouse model using two-dimensional polyacrylamide gel electrophoresis (2-D PAGE) [13]. Other researchers have shown that main proteins that exhibited changes in expression in mouse heart failure models belong to specific functional categories, including myocardial proteins, signal transduction proteins, metabolism-related proteins, transcriptional and translational proteins, growth and proliferation proteins and proteins with unknown function [14–16]. Although several studies have identified specific pathways that may be involved in heart failure [17–18], few have taken a global approach to identify key components of heart disease pathogenesis, especially using proteins extracted from the failing human heart. Through proteomic

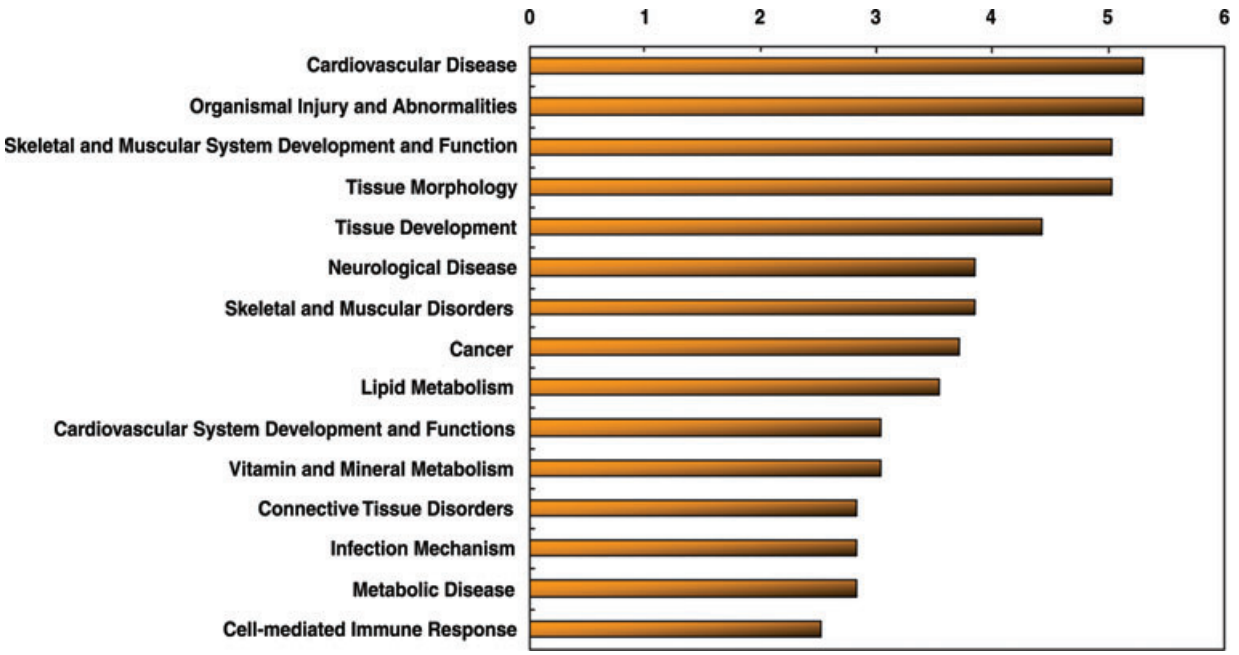

Fig. 3 Functional characterisation of proteins detected to display aberrant expression across the failing heart. The gene list was imported and analysed by the Core Analysis Module in IPA software to statistically determine the functions/pathways most strongly associated with the gene list.

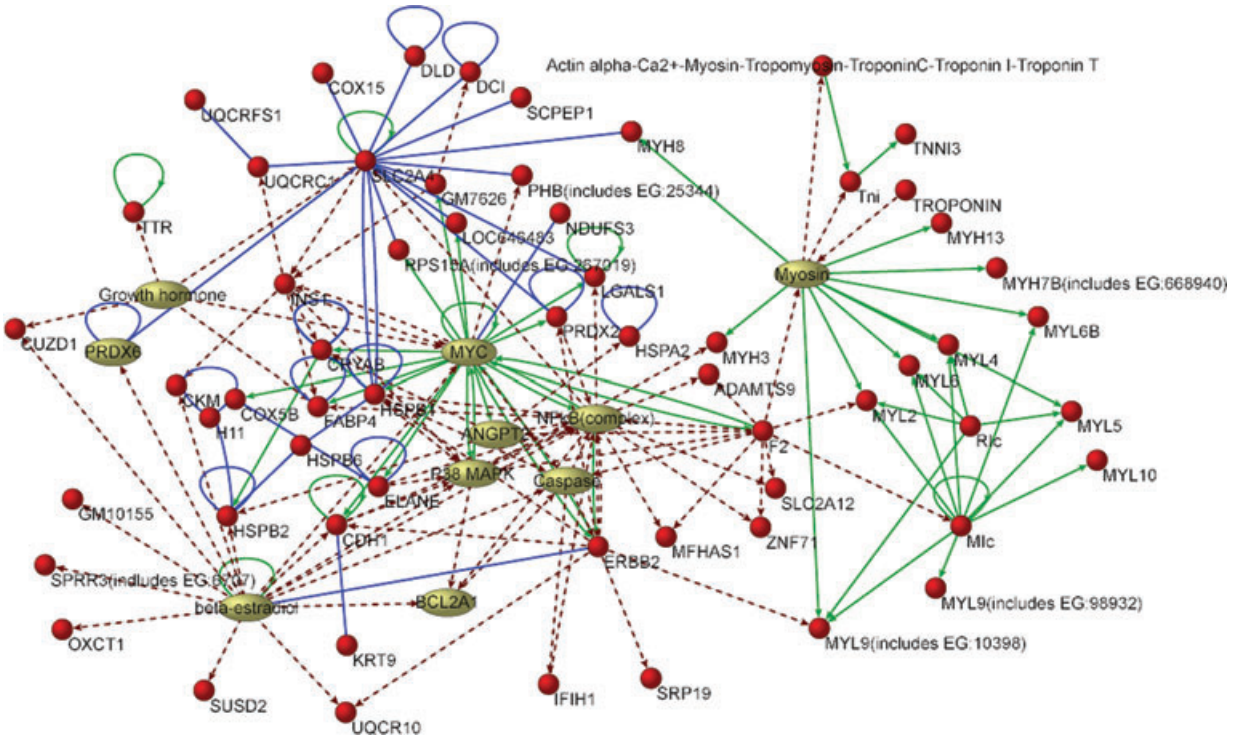

Fig. 4 The network analysis of proteomics using IPA. The top list of several pathways by this enrichment analysis are highlighted, such as NF-κB, TGF-β and P38-MAPK signalling pathways demonstrate to play an important role in the mechanical signalling during heart failure, Besides, several metabolism disease pathways, including Growth Hormone and PRDX6 pathway, are also highlighted. Meanwhile, functional modules related to cell differentiation and proliferation, as well as apoptosis (caspases) are centred in the interaction network including only experimentally validated targets. Moreover, some important modulators in immune/inflammatory response, cardiovascular development or angiogenesis, including TTR, ANGPT2 and FABP can also be found in the interaction map. The arrows represent the regulation between two proteins.

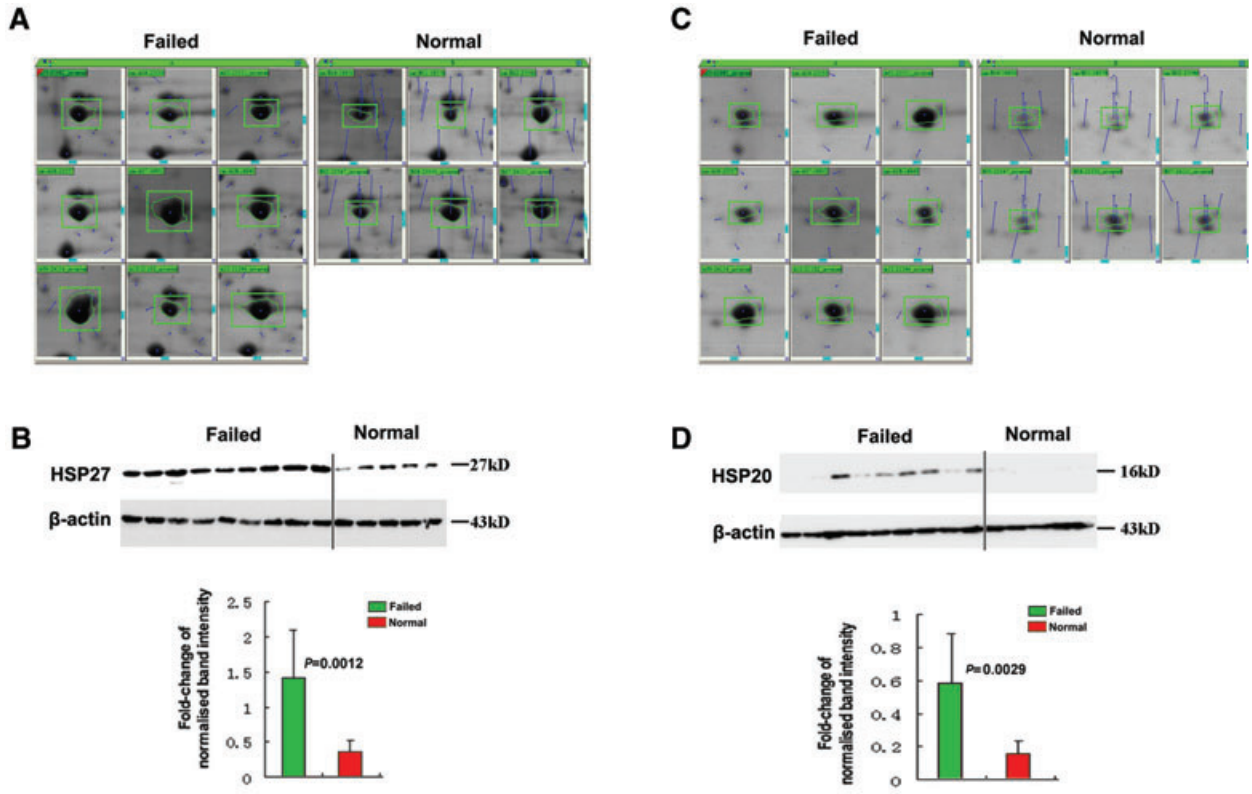

Fig. 5 Changes in the protein expression of HSP27 and HSP20 determined by Western blot analysis of ventricular tissues from failed and normal hearts. Detailed 2-DE images of altered proteins (**A**, **C**) and Western blot analysis (**B**, **D**). Expression of HSP27 and HSP20 was increased in failed compared with normal hearts (fold change = 4, $P = 0.0012$; fold change = 3, $P = 0.0029$, respectively). β-Actin expression was used as a loading control.

analysis, we have carried out a full-scale screen of the protein changes in human heart failure, which mainly refer to several functional protein groups: proteins involved in mitochondria and energy metabolism, proteins involved in cardiac muscle contraction and others.

Mitochondrial and energy metabolism proteins

The proteins located within the mitochondria or involved in processes of energy metabolism play an important role in the heart's metabolic function. The main way that myocytes compensate for decreasing mitochondrial function is by increasing the expression of glycolysis-related proteins [19]. Therefore, high rates of myocardial energy production are required to maintain the constant demand of the working heart for adenosine triphosphate (ATP) and key enzymes involved in the Krebs cycle [20].

A total of seven proteins involved in the tricarboxylic acid cycle and respiratory activities change. Pronounced changes in key enzymes that regulate oxidation processes have often been revealed in subunits of electron transport chain complexes [21, 22]. These structures are embedded in the inner mitochondrial membrane and facilitate the transfer of electrons, creating a proton gradient across the myocyte membrane, completing the generation of energy from adenosine diphosphate (ADP) to ATP. A recent study described a reduction in activity and expression during the development of cardiac hypertrophy in rats, supporting the relevance of mitochondrial membrane proteins as an early and persistent marker of oxidative stress-related mitochondrial alterations in the development of hypertrophy [23].

Our results (Tables 2 and 3) indicate that comparison of the proteome of the failing heart with that of the normal heart identified changes in expression of four protein subunits from the following four respiratory complexes: (i) Complex I: NADH dehydrogenase (ubiquinone) Fe-S protein 3; (ii) Complex II: dihydrolipoamide dehydrogenase; (iii) Complex III: cytochrome *c* oxidase subunit Vb and (iv) Complex IV: dodecenoyl-Coenzyme A delta isomerase (3,2 trans-enoyl-Coenzyme A isomerase). These data imply the membrane microdomains could be a platform to integrate chemiosmosis as well as oxidation/reduction reactions. Therefore, the increased proteins that are the pronounced enzymes in the respiratory process can be explained by an increased demand for energy by unsynchronized changes in dysfunctional myocytes [24]. This conclusion is in concordance with

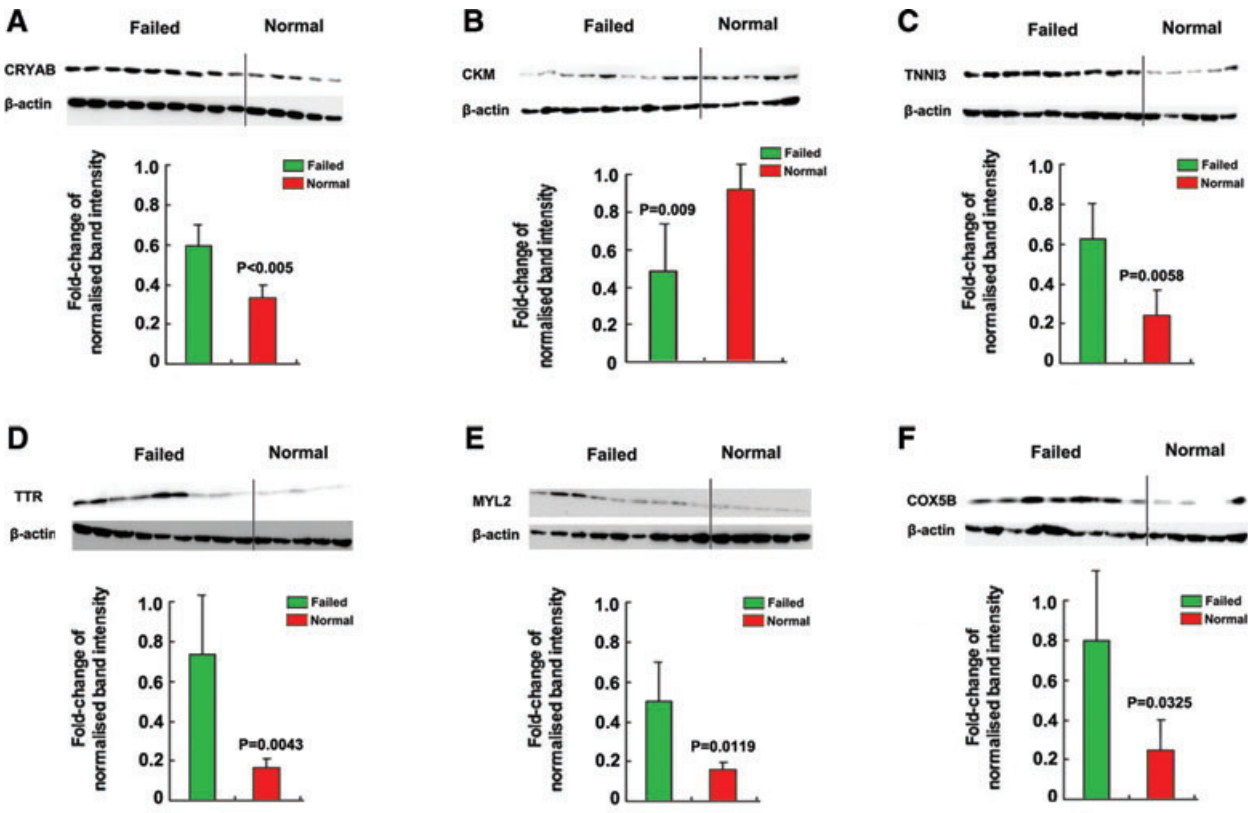

Fig. 6 Confirmative Western blot assays for selected proteins. Sucrose gradient fractions were separated by 12% SDS-PAGE and transferred to the NC membrane, and hybridized with anti-CRYAB (**A**), anti-CKM (**B**), anti-TNNI3 (**C**), anti-TTR (**D**), anti-MYL-2 (**E**) and anti-COX5B (**F**) antibodies. The bar graph shows the relative spot densities. CRYAB: crystallin, αB; CKM: creatine kinase, muscle; TNNI3: troponin I type 3 (cardiac); TTR: transthyretin; MYL-2: myosin, light chain 2; COX5B: cytochrome *c* oxidase subunit Vb.

studies of cardiac hypertrophy in non-failing hearts in pressure-overload-induced hypertrophy models [25].

Cardiac muscle cell contraction

Our study indicates proteins involved in cell structure and muscle contraction also represent a large proportion of the expression proteins in the failing human heart. Seven cytoskeletal proteins with marked increases in expression are grouped in this category, including myosin light chain proteins, troponin I type 3 and transthyretin. Myosin light chain proteins are essential components in generating actin-based contractile force, and alterations in the expression of these proteins could affect myocardial contractility [26, 27].

It has already been identified that the genetic ablation of the N-terminal myosin essential light chain extension induces reduced force per cross-sectional area of muscle and leads to age-dependent compensatory cardiac hypertrophy [28]. Specifically, changes in myosin light chain 2 protein expressions have been linked to contractile dysfunction in dilated cardiomyopathy [29], ischaemia/reperfusion injury [30] and heart failure [31]. The up-regulation of these proteins in the failing human heart may indicate compensatory mechanisms due to adaptive response to the decrease of cardiac actin. Moreover, changes in myosin light chain 2 expression observed in this study may represent a shift in phosphorylation or deamidation rather than an overall increase in expression. Recent research shows that 50% mutant myosin regulatory light chain causes mechanical dysfunction of muscle fibres by sufficiently perturbing the tension at subsaturating Ca^{2+} concentrations; calcium sensitivity and cooperativity of force generation of fibres may be directly linked to the mechanism for familial hypertrophic cardiomyopathy [32].

Another important protein is Troponin I isoform TNNI3 (TNNI3), a constituent protein of the troponin complex located on the thin filament of striated muscle. TNNI3 provides a calcium-sensitive switch for striated muscle contraction and has the ability to regulate systemic arterial blood pressure with respect to ischaemic conditions. TNNI3 takes part in the regulation of cardiac muscle contraction and ventricular cardiac muscle tissue

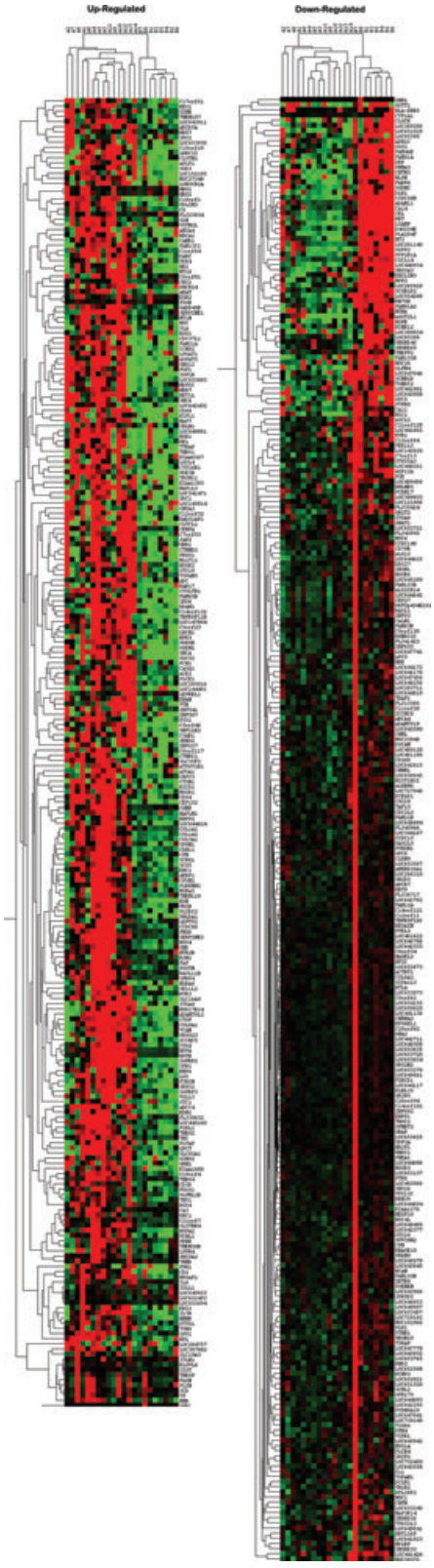

Fig. 7 Heatmap of mRNA microarray expression data from heart samples of heart failure patients ($n = 14$) and healthy controls ($n = 8$). These genes were derived from 2-way ANOVA, false discovery rate multiple comparisons correction were less than or equal to 5%. These dysregulated genes were hierarchically clustered on the *Y*-axis, and patient samples or healthy control samples were hierarchically clustered on the *X*-axis. The legend on the right indicates the genes represented in the corresponding row. The relative expression of mRNA is depicted according to the colour scale shown on the right. Red indicates up-regulated and blue indicates down-regulated genes.

Table 4 The expression levels of mRNAs of altered proteins by using microarray in failed group compared to control group

	Heart failure ($n = 14$)	Control ($n = 8$)	Fold change	*P* value*
HSP20 (HSPB6)	5796.445	3005.389	1.928683	0.349
COX5B	8882.66	10863.76	0.8176411	1
CRYAB	20202.15	19992.46	1.010488	1
LGALS1	4213.337	4256.731	0.9898058	1
MYL2	33942.31	36326.29	0.9343731	1
HSPB2	646.0505	743.0538	0.8694531	1
MYL6	5329.922	4815.298	1.106873	1
DLD	1058.641	922.835	1.147162	1
OXCT1	624.9647	436.0639	1.433195	1
FABP4	562.7787	395.8654	1.421641	1
PRDX6	3072.933	2949.509	1.041846	1
HSPA2	396.8911	83.09702	4.776237	0.044
TNNI3	5090.322	5438.007	0.9360639	1
TTR	28.36996	40.90046	0.6936343	1
HSP27 (HSPB1)	6059.404	5597.423	1.082535	1
BCL2A1	2.169603	1.955042	1.109747	1
CKM	15383.75	16266.23	0.9457479	1
IFIH1	85.44498	76.69858	1.114036	1
KRT9	25.62142	72.2167	0.3547852	1
DCI	359.5333	464.1664	0.7745785	1
NDUFS3	2959.224	3386.83	0.8737445	1
PRDX2	1318.944	1411.478	0.9344414	1
SRP19	311.3288	336.2429	0.9259046	1
MYL4	897.3405	1503.386	0.5968796	1
UQCRFS1	9222.257	9154.988	1.007348	1

* *P* value was calculated by illumina custom error model implemented in GenomeStudio and corrected by Benjamini-Hochberg False Discovery Rate.

morphogenesis. It binds actin and inhibits actomyosin ATPase activity in the absence of activating levels of calcium [33]. Proteins related to changes in cardiac muscle contraction in response to cellular calcium ion homeostasis may be another important pathway in the development of heart failure.

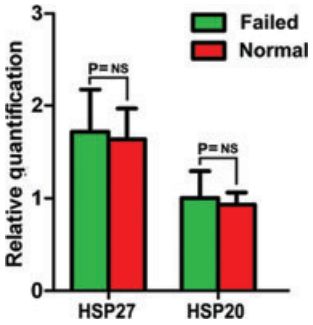

Fig. 8 Real-time reverse transcriptase PCR analysis of mRNA expression of HSP27 and HSP20. The relative expression of HSP27 (**A**) and HSP20 (**B**) in failed compared with normal hearts was normalized to β-actin expression. *P* values were calculated by two-sided Student's *t*-test.

Others

Our study investigates some highly expressed proteins that maintain both morphologic and functional integrity of cardiomyocytes and increase tolerance against various types of stress, including αB-crystallin, HSP27 and HSP20 [34–36].

HSPs fulfil a wide range of functions, including cytoprotection and the intracellular assembly, folding and translocation of oligomeric proteins, and also represent a rapid response to altered redox states [37]. Failure to increase the levels of these high molecular HSPs may represent a loss of compensatory responsiveness in the setting of heart failure [38]. The highly expressed small HSPs (smHSPs) may exert effects on the left ventricular remodelling process that are different from those of high molecular HSPs, and it may be important to investigate the expression levels of smHSPs to better understand the pathogenesis of heart failure [39]. αB-crystallin is an smHSP structurally related to other smHSPs including αA-crystallin, HSP27, HSP20, HSP22, myotonic dystrophy protein kinase binding protein and HSPB3 [40]. αB-crystallin has strong anti-apoptotic properties and, when fully induced, is the most abundant smHSP in the heart and may constitute as much as 5% of total cardiac myocyte protein. It has been proposed that chaperoning by αB-crystallin can stabilize myofilament proteins through selective interactions with actin, titin, nebulette and the intermediate filaments desmin and vimentin [41]. With the compromise of αB-crystallin function, abnormal desmin forms aberrant aggregates and disrupts the integrity of the desmin network, which causes a reduction in cardiac function [42, 43].

An interesting finding in our study is the down-regulation of BCL2A1 (often named bfl-1) in patients with heart failure. There is not much known about the role of BCL2A1 in cardiac function and the implication in heart failure. Like many members of BCL2 family, BCL2A1 contains both pro- and anti-apoptotic properties depending on its intracellular localization [44, 45]. In a mouse model that mimics the mitochondrial DNA mutation–induced dilated cardiomyopathy, it has been shown that BCL2A1 and HSP27 are up-regulated as a compensatory mechanism to protect against apoptosis [46]. Therefore, it may be possible that the low levels of BCL2A1 are associated with the increased cell death during the heart failure. More research needs to be done to fully understand the biological roles of BCL2A1 that influence the course and outcome of heart failure.

In this study, human heart tissues were used to find that major protein changes in heart failure pathogenesis can be grouped into proteins involved in mitochondria and energy production and cytoskeleton proteins. Further studies of these proteins and pathways during the end-stage heart failure are necessary to address their precise roles in the pathophysiology of heart failure and their potential as diagnostic tools or therapeutic targets. This study has raised numerous questions and opened several new avenues for the future study of this complex disease.

Acknowledgements

This work is supported by grants from the National Science Foundation of China (Nos. 81050012, 30888004 and 30900590), Beijing Nova Program (No. 2009B39), Beijing Natural Science Foundation (No. 7102057) and the Scientific Research Foundation for the Returned Overseas Chinese Scholars, Education Ministry of China.

Conflict of interest

The authors confirm that there are no conflicts of interest.

References

1. **Adams Jr K, Baughman K, Dec W, *et al.*** HFSA guidelines for management of patients with heart failure caused by left ventricular systolic dysfunction-pharmacological approaches. *Pharmacotherapy.* 2000; 20: 495–2.
2. **Stewart S, MacIntyre K, Capewell S, *et al.*** Heart failure and the aging population: an increasing burden in the 21st century? *Heart.* 2003; 89: 49–3.
3. **Wasinger V, Cordwell S, Cerpa-Poljak A, *et al.*** Progress with gene-product mapping of the mollicutes: mycoplasma genitalium. *Electrophoresis.* 1995; 16: 1090–4.
4. **Fink J, Aturaliya R, Davis M, *et al.*** Locate: a mouse protein subcellular localization database. *Nucleic Acids Res.* 2006; 34: D213–7.
5. **Thomas P, Campbell M, Kejariwal A, *et al.*** Panther: a library of protein families and subfamilies indexed by function. *Genome Res.* 2003; 13: 2129–41.
6. **Van der Heiden K, Cuhlmann S, Luong le A, *et al.*** Role of nuclear factor kappaB in cardiovascular health and disease. *Clin Sci.* 2010; 118: 593–5.
7. **Lee HG, Chen Q, Wolfram JA, *et al.*** Cell cycle re-entry and mitochondrial defects in myc-mediated hypertrophic cardiomyopathy and heart failure. *PLoS One.* 2009; 4: e7172.

8. **Lemke LE, Bloem LJ, Fouts R, *et al.*** Decreased p38 MAPK activity in end-stage failing human myocardium: p38 MAPK alpha is the predominant isoform expressed in human heart. *J Mol Cell Cardiol*. 2001; 33: 1527–40.
9. **Fatma N, Kubo E, Takamura Y, *et al.*** Loss of NF-kappaB control and repression of Prdx6 gene transcription by reactive oxygen species-driven SMAD3-mediated transforming growth factor beta signaling. *J Biol Chem*. 2009; 284: 22758–72.
10. **Janunger T, Anan I, Holmgren G, *et al.*** Heart failure caused by a novel amyloidogenic mutation of the transthyretin gene: ATTR Ala45Ser. *Amyloid*. 2000; 7: 137–40.
11. **Fiedler U, Reiss Y, Scharpfenecker M, *et al.*** Angiopoietin-2 sensitizes endothelial cells to TNF-alpha and has a crucial role in the induction of inflammation. *Nat Med*. 2006; 12: 235–9.
12. **Niizeki T, Takeishi Y, Arimoto T, *et al.*** Heart-type fatty acid-binding protein is more sensitive than troponin T to detect the ongoing myocardial damage in chronic heart failure patients. *J Card Fail*. 2007; 13: 120–7.
13. **Lam L, Arthur J, Semsarian C.** Proteome map of the normal murine ventricular myocardium. *Proteomics*. 2007; 7: 3629–33.
14. **Fountoulakis M, Soumaka E, Rapti K, *et al.*** Alterations in the heart mitochondrial proteome in a desmin null heart failure model. *J Mol Cell Cardiol*. 2005; 38: 461–74.
15. **Wei Y, Cui C, Lainscak M, *et al.*** Type-specific dysregulation of matrix metalloproteinases and their tissue inhibitors in end-stage heart failure patients. *J Cell Mol Med*. 2010; 15: 773–82.
16. **Chen JF, Murchison EP, Tang R, *et al.*** Targeted deletion of Dicer in the heart leads to dilated cardiomyopathy and heart failure. *Proc Natl Acad Sci USA*. 2008; 105: 2111–6.
17. **Schipper ME, van Kuik J, de Jonge N, *et al.*** Changes in regulatory microRNA expression in myocardium of heart failure patients on left ventricular assist device support. *J Heart Lung Transplant*. 2008; 27: 1282–5.
18. **Predmore JM, Wang P, Davis F, *et al.*** Ubiquitin proteasome dysfunction in human hypertrophic and dilated cardiomyopathies. *Circulation*. 2010; 121: 997–1004.
19. **Heinke M, Wheeler C, Chang D, *et al.*** Protein changes observed in pacing-induced heart failure using two-dimensional electrophoresis. *Electrophoresis*. 1998; 19: 2021–30.
20. **Sawicki G, Jugdutt B.** Detection of regional changes in protein levels in the *in vivo* canine model of acute heart failure following ischemia-reperfusion injury: functional proteomics studies. *Proteomics*. 2004; 4: 2195–202.
21. **Chu G, Kerr J, Mitton B, *et al.*** Proteomic analysis of hyperdynamic mouse hearts with enhanced sarcoplasmic reticulum calcium cycling. *FASEB J*. 2004: 04: 1725–7.
22. **Jüllig M, Hickey A, Chai C, *et al.*** Is the failing heart out of fuel or a worn engine running rich? A study of mitochondria in old spontaneously hypertensive rats. *Proteomics*. 2008; 8: 2556–72.
23. **Weekes J, Wheeler C, Yan J, *et al.*** Bovine dilated cardiomyopathy: proteomic analysis of an animal model of human dilated cardiomyopathy. *Electrophoresis*. 1999; 20: 898–906.
24. **Ashrafian H, Redwood C, Blair E, *et al.*** Hypertrophic cardiomyopathy: a paradigm for myocardial energy depletion. *Trends Genet*. 2003; 19: 263–8.
25. **Jin X, Xia L, Wang L, *et al.*** Differential protein expression in hypertrophic heart with and without hypertension in spontaneously hypertensive rats. *Proteomics*. 2006; 6: 1948–56.
26. **Ogut O, Brozovich F.** The potential role of MLC phosphatase and MAPK signalling in the pathogenesis of vascular dysfunction in heart failure. *J Cell Mol Med*. 2008; 12: 2158–64.
27. **Seguchi O, Takashima S, Yamazaki S, *et al.*** A cardiac myosin light chain kinase regulates sarcomere assembly in the vertebrate heart. *J Clin Invest*. 2007; 117: 2812–24.
28. **Kazmierczak K, Xu Y, Jones M, *et al.*** The role of the n-terminus of the myosin essential light chain in cardiac muscle contraction. *J Mol Biol*. 2009; 387: 706–25.
29. **Corbett J, Why H, Wheeler C, *et al.*** Cardiac protein abnormalities in dilated cardiomyopathy detected by two-dimensional polyacrylamide gel electrophoresis. *Electrophoresis*. 1998; 19: 2031–42.
30. **White M, Cordwell S, McCarron H, *et al.*** Proteomics of ischemia/reperfusion injury in rabbit myocardium reveals alterations to proteins of essential functional systems. *Proteomics*. 2005; 5: 1395–410.
31. **Van der Velden J, Papp Z, Boontje N, *et al.*** The effect of myosin light chain 2 dephosphorylation on Ca^{2+}-sensitivity of force is enhanced in failing human hearts. *Cardiovasc Res*. 2003; 57: 505–14.
32. **Roopnarine O.** Mechanical defects of muscle fibers with myosin light chain mutants that cause cardiomyopathy. *Biophys J*. 2003; 84: 2440–9.
33. **Bhavsar P, Brand N, Yacoub M, *et al.*** Isolation and characterization of the human cardiac troponin I gene (TNNI3). *Genomics*. 1996; 35: 11–23.
34. **Fan G, Chu G, Mitton B, *et al.*** Small heat-shock protein hsp20 phosphorylation inhibits beta-agonist-induced cardiac apoptosis. *Circ Res*. 2004; 94: 1474–82.
35. **Haslbeck M.** sHsps and their role in the chaperone network. *Cell Mol Life Sci*. 2002; 59: 1649–57.
36. **Martin J, Mestril R, Hilal-Dandan R, *et al.*** Small heat shock proteins and protection against ischemic injury in cardiac myocytes. *Circulation*. 1997; 96: 4343–8.
37. **Chi N, Karliner J.** Molecular determinants of responses to myocardial ischemia/reperfusion injury: focus on hypoxia-inducible and heat shock factors. *Cardiovasc Res*. 2004; 61: 437–47.
38. **Knowlton A, Kapadia S, Torre-Amione G, *et al.*** Differential expression of heat shock proteins in normal and failing human hearts. *J Mol Cell Cardiol*. 1998; 30: 811–8.
39. **Dohke T, Wada A, Isono T, *et al.*** Proteomic analysis reveals significant alternations of cardiac small heat shock protein expression in congestive heart failure. *J Cardiac Fail*. 2006; 12: 77–84.
40. **Webster K.** Serine phosphorylation and suppression of apoptosis by the small heat shock protein αB-crystallin. *Circ Res*. 2003; 92: 130–2.
41. **Banfi C, Brioschi M, Wait R, *et al.*** Proteomic analysis of membrane microdomains derived from both failing and non-failing human hearts. *Proteomics*. 2006; 6: 1976–88.
42. **Vicart P, Caron A, Guicheney P, *et al.*** A missense mutation in the αB-crystallin chaperone gene causes a desmin-related myopathy. *Nat Genet*. 1998; 20: 92–5.
43. **Wang X, Klevitsky R, Huang W, *et al.*** AlphaB-crystallin modulates protein aggregation of abnormal desmin. *Circ Res*. 2003; 93: 998–1005.
44. **D'Sa-Eipper C, Subramanian T, Chinnadurai G.** Bfl-1, a bcl-2 homologue, suppresses p53-induced apoptosis and exhibits potent cooperative transforming activity. *Cancer Res*. 1996; 56: 3879–82.
45. **Zong WX, Edelstein LC, Chen C, *et al.*** The prosurvival Bcl-2 homolog Bfl-1/A1 is a direct transcriptional target of NF-κB that blocks TNF-α–induced apoptosis. *Genes Dev*. 1999; 13: 382–7.
46. **Zhang D, Mott JL, Farrar P, *et al.*** Mitochondrial DNA mutations activate the mitochondrial apoptotic pathway and cause dilated cardiomyopathy. *Cardiovasc Res*. 2003; 57: 147–57.